GEOLOGICAL SURVEY OF CANADA
OPEN FILE 6283

Thermal Remote Sensing of Urban Heat Island Effects: Greater Toronto Area

M.J. Maloley

2010

Natural Resources Canada | Ressources naturelles Canada

Canada

GEOLOGICAL SURVEY OF CANADA
OPEN FILE 6283

Thermal Remote Sensing of Urban Heat Island Effects: Greater Toronto Area

M.J. Maloley

2010

This publication is available from the Geological Survey of Canada Bookstore
(http://gsc.nrcan.gc.ca/bookstore_e.php).
It can also be downloaded free of charge from GeoPub
(http://geopub.rncan.gc.ca/).

Maloley, M.J. 2010. Thermal Remote Sensing of Urban Heat Island Effects: Greater Toronto Area; Geological Survey of Canada, Open File 6283, 39 p.

Open files are products that have not gone through the GSC formal publication process.

Table of Contents

Acknowledgements

Initial planning and guidance for this research activity was provided by Dr. Ying Zhang and Dr. Bert Guindon. The field work, imagery processing and analysis were supported by Lixin Sun, Raymond Soffer, Emma Hemmingsen and Amy Gartshore. This research would not have been possible without the support of the Clean Air Partnership (CAP), which facilitated unprecedented access to urban sites for field measurements. Virginia Mersereau, and Dr. Jennifer Penney from CAP also provided valuable scientific direction and acted as key liaisons with the City of Toronto and other stakeholders.

This research also depended heavily on meteorological station data from independent sources and we'd like to extend our gratitude for data access to City of Toronto, University of Toronto, York University, Toronto Regional Conservation Authority and Ministry of Transportation Ontario.

Jennifer Forkes, Dr. Bert Guindon and Dr. Robert Gauthier are thanked for their critical review of the report. Finally, the author would like to acknowledge the support and encouragement of some key managers, specifically David Mate and Jean-Marc Chouinard.

1. Introduction

This report presents the results from the ESS research activity 'Assessment of Urban Heat Island Impacts in GTA Region'. It was part of the *Building Capacity for Climate Change in Canadian Communities* project in the ESS Climate Change Geoscience program. The goals of the research activity are to contribute earth science information to improve understanding of the urban heat island (UHI) effects and to support development of effective planning strategies related to urban development, hot weather response and energy consumption within the context of a warming climate. A central theme of the activity was the use of Earth Observation (EO) technologies to estimate temperatures to characterize urban heat of the Greater Toronto Area (GTA) region.

Populations living in UHIs can be more vulnerable to extreme heat events (Oke, 1987). Extreme heat events are a health risk as demonstrated by the excess mortality in urban areas recorded during the heat wave in France in 2003 (Fouillet et al., 2006). With 80% of Canadians living in urban areas and a projected increase in extreme heat events (Natural Resources Canada, 2007), there is a clear public health requirement for UHI mapping and monitoring. Decision makers who are developing and implementing measures to mitigate impacts of extreme heat events would benefit greatly from knowing the locations where people are most likely to be exposed to high temperatures.

Preliminary studies suggested that remote sensing offers the potential to map surface temperatures and subsequently characterize UHIs, however there are limitations in the estimation of actual air temperatures (Roth et al., 1989, Voogt and Oke, 2003). In order to address these limitations, three research objectives were defined to guide the activity:

(1) To investigate the relationships between surface temperature, air temperature and remotely sensed surface temperature.
(2) To investigate the relationships between in situ and remotely observed surface temperatures of different urban surface covers.
(3) To investigate the spatial and temporal scales of urban heat fluxes and whether existing remote sensing platforms are appropriate for characterizing these measurements.

In order to meet these objectives, Landsat TM and ETM+ images between 1987 and 2008 were acquired and used to produce Land Surface Temperature (LST) maps. Using over 20 years of imagery allows the detection of changes in urban surface temperatures as a result of urbanization, and of the temporal persistence of hot/cool spots. A field campaign was carried out to collect in situ air and surface temperatures during the summers of 2007 and 2008. The purpose of the field campaign would both serve to validate the LST maps, and to provide data on the diurnal variations of surface and air temperatures of various urban covers. Various other geospatial information (i.e. Land Cover) was also incorporated into the study to address the research objectives.

2. Background

2.1. Urban Heat Islands

Urban centres tend to have higher air temperatures than surrounding rural areas as a result of vegetated cover being replaced by non-porous, non-evaporating, high thermal inertia surfaces such as concrete and asphalt. In addition to differences in land cover, urban areas tend to have greater surface roughness, which limits wind speeds and therefore reduces urban cooling .Another contributing factor to the UHI is the urban canyon effect, where walls of multi-storey buildings release heat that has been stored from daytime heating at lower rates during periods of nighttime cooling than non-urban features (Oke, 1982). In many cases (i.e. arid rural areas), the peak diurnal difference in urban and rural air temperatures is not found at solar noon but instead during nocturnal cooling periods, suggesting that impervious cover is not the dominant control of the UHI effect but instead the urban canopy (Peña, 2008; Oke, 1981).

The UHI effect is commonly described by its UHI intensity (ΔT_{u-r}), which is measured as the difference in air temperature between an urban area (u) and its rural surround (r). The UHI effect is normally measured within the urban canopy layer (UCL), which extends from the ground to the mean roof or treetop height. The rural site is assumed to be the control site. True independence for the rural control and urban test sites is difficult to establish as all sites need similar macro-climatic conditions (i.e. total incoming radiation, prevailing winds, lake effects) and yet be distant enough from each other that they do not receive any additional boundary layer[1] heating. Typically the spatial distribution of UHI intensity generally shows maximum differences at the urban center with a large temperature gradient at the urban-rural edge. Larger UHI intensities are typically found when measuring surface temperature differences rather than air temperatures differences.

Surface temperature is critical to urban climatology. It determines the air temperature of the urban atmosphere and is central to the energy balance at the surface. However, in terms of UHI and human health, it is the air temperature which not only affects comfort, but in extreme heat events, determines mortality and morbidity (Smargiassi et al., 2007). Surface and air temperatures are not directly correlated, particularly over the diurnal temperature cycle and their relationship can vary considerably with winds and humidity.

[1] The urban boundary layer (UBL) is the mesoscale boundary layer, which combines the cumulative effect of the energy budget from the city beneath and the atmosphere.

2.2. Thermal Remote Sensing

2.2.1. Estimating Land Surface Temperature from Thermal Imagery

Thermal remote sensors (i.e. Landsat TM and ETM+) capture spatially extensive per-pixel estimates of radiated energy in the 10.4-12.5 µm spectrum. Effectively, the energy radiated in this spectral range can be directly related to radiant temperature of the earth's surface.

To estimate LST from satellite thermal data, the digital number (DN) of each image pixel is converted into spectral radiance using the sensor calibration data (Markham and Barker, 1986). The spectral radiance value can then be converted to represent surface temperature.

There are, however, some potential sources of error. First, the digital number may include other fractions of energy, which may introduce error into the estimate. In addition to radiation emitted from the ground, there may be upwelling radiance from the atmosphere, as well as downwelling radiance from the sky integrated over the hemisphere above the surface. These other sources of radiation can introduce error into the estimation of surface temperature.

A second factor that must be considered in the estimation of surface temperatures of urban areas from satellite imagery, is what surface is actually being "seen" by the sensor. With complex 3D urban structures, there is a directional component to both how walls and roofs heat up or are shaded from solar radiation and how they are observed by the satellite sensor which may be off-nadir (Voogt and Oke, 1998). The sensor view angle of Landsat based thermal measurements is at nadir. However there is still a biased view of surface temperatures due to the orientation of the urban surface facets to the sun at 10:00 . In this study, this effect is likely to be considerable for the downtown core of the GTA, where Landsat may detect cool shaded rooftops while omitting warm building walls, leading to a possible underestimation of the total radiated heat in a single pixel area.

Numerous algorithms have been tested to convert the calibrated thermal radiance to LST (Schott and Volchol, 1985; Goetz et al., 1995, Sobrino et al. 2004). The majority of these methods perform well, with errors below 2.0°C, but require extensive atmospheric corrections and spatially explicit information on surface emissivities. Effectively, to obtain surface temperatures to an accuracy of 0.1°C, the emissivity must be known to within 0.1% (Stroeve et al., 1996). Under uniform land cover with small variations in emissivities, this level of accuracy is possible. However, emissivities can vary considerably over urban cover (0.96-0.99%) (Snyder et al., 1998), and estimating emissivity is difficult even with extensive land cover information. Axelsson and Lunden (1988) present the difficulties in estimating emissivities for heterogeneous urban areas, however, Sobrino et al. (2004) are

able to demonstrate improved accuracies in LST estimation in non-urban areas by using emissivity information. Based on the heterogeneity of the GTA, particularly considering the mix of urban cover types within a 60 or 120 m Landsat pixel, in this study, the production of LST maps employed a method that assumed all pixels to have a uniform emissivity, accepting error within the 2.0°C range.

Once per-pixel LST estimates have been calculated, their use is still limited in terms of analyzing the effects of land use change on surface temperature. Although the timing of the acquisitions are controlled (e.g. every 16 days), the climate conditions are not. Current radiative conditions, such as sun angle, cloud cover and haze, as well as antecedent conditions such as rainfall which may have altered the moisture content of pervious surfaces, influence surface temperatures on any given acquisition. The comparison of surface temperatures from multiple dates can be uninformative if the microclimate conditions under which the various images were acquired are different. In order to address these limitations, LST may need to be calibrated to a standard thermal regime for direct comparison.

2.2.2. Landsat Sensors

The Landsat sensors have a relatively high spatial resolution (120 m for TM and 60 m for ETM+), capturing swaths of 185 km with 16 day repeat cycles at approximately 10:00 local time. Landsat TM has been operational since March 1, 1984 and with a 25 year record of imagery. Landsat ETM+ has been operational since April 15, 1999, however on May 31, 2003 the Scan Line Corrector (SLC) instrument failed. The SLC failure results in linear gaps of missing data within the acquired image (i.e. 5 pixel gaps every 15 pixels). Data is still being collected despite this error, allowing the possibility to produce incomplete LST maps.

The Landsat thermal sensors have been calibrated extensively by NASA and USGS with regular updates for the radiometric calibration parameters (gain and offset) that are necessary to properly calculate radiance (Barsi et al., 2003). Both TM and ETM+ sensors have on-board thermal calibration systems consisting of blackbody and low emissive shutters. Tests have also been carried out using both the on board calibration systems and surface targets with known temperatures and emissivities to validate these sensor calibrations (Barsi et al., 2003).

3. Methods

3.1. Study Area

The study area, which includes the GTA as well as the rural fringe as far north as the Oak Ridge Moraine, covers roughly 200 km^2. The GTA was selected as the study area because of its extensive urban cover and observed UHI effect. The GTA has also undergone significant land cover change over the past 20 years, particularly as areas of intense urbanization. These changes should present multi-year variations in UHI intensity. The study area extent and in situ measurement locations are shown in Figure 1. The urban study site may also be representative of other North American metropolitan areas, with its distinct central business district and substantial residential periphery. However, considerations should be made for the city's proximity to Lake Ontario, which will likely contribute to the microclimatology of both urban and rural areas.

3.2. In situ Surface and Air Temperature Monitoring Sites

During the summers of 2007 and 2008, in situ measurements were collected at 40 monitoring sites across the GTA study area covering wide range of urban surface covers. (*Measurement site details can be found in Appendix I.*)

In many cases monitoring sites were installed on rooftops, but all measurements were assumed to be made within the UCL. However, there was an expected bias due to some temperature sensors being located at "street" or ground level.

The monitoring site specifications varied among many of the sites due to individual site properties and the equipment employed. However, some minimum specifications were met for each site. At each site, air temperature was measured at a minimum of every hour at approximately 1.5 m above the surface. Each of the 26 NRCan monitoring sites, selected with the assistance of the Clean Air Partnership (CAP), had air temperature, and in many cases collocated surface temperature, sensors installed on and over the dominant surface covers.

Other monitoring sites included meteorological stations from Environment Canada, Toronto Regional Conservation Authority (TRCA) and Ontario Ministry of Transportation. At these sites, a wide range of measurements, including wind speed, precipitation and solar radiation, were collected during the study. Additional meteorological data was acquired from monitoring at the University of Toronto and York University. While the 40 sites provided data for a many of the dominant urban surface covers, there were large spatial gaps between sites (i.e. 10km) and certain surface cover types were not included due to access (e.g. private businesses) or security reasons (e.g. parks).

The breakdown of stations by land use is as follows; 26 urban, 8 rural, 6 suburban. Two of the urban sites were also classified as “green roofs” with drought resistant vegetation. Photos of typical monitoring installations for surface and air temperatures at the NRCan sites can be seen in Figure 2.

3.2.1. Temperature Measurement Continuity and Pre-Processing

Maintenance of the monitoring station network involved removing or re-locating stations based on site access or initial results that indicated redundancy. Access to many of the stations was extremely difficult and ultimately resulted in a number of sensor outages due to battery failures or undetected failure or damage over long periods. Based on the outages and varied site specifications, there were only a few time periods of data acquisitions during which most stations were operating.

All temperature measurements were averaged to hourly data points to meet the coarsest requirements of recording frequency. Initial analysis indicated that there was little impact on temperature variability that was being smoothed over by using hourly averages.

3.2.2. Measurement Validation

The NRCan HOBO TMC-HD air temperature sensors were tested but not validated prior to installation at the monitoring sites. Instead, during installation, the sensor readings were compared to portable Digisense temperature sensor measurements (±0.2°C listed accuracy) carried by the field crews. All of the installed temperature sensors recorded differences no greater than ±0.5° C with the Digisense measurements. A brief quality control was carried out on the collected data through comparisons of maximum hourly differences between the NRCan air temperature data and a control at the Environment Canada Lester B. Pearson Airport station. Temperature differences exceeding 5°C would likely indicate an erroneous measurement as opposed to actual site difference. No stations reported more than 4.8°C differences over the comparison period and were deemed valid.

As the NRCan surface temperature sensors were customized thermistors for point contact measurements, a pre-deployment validation procedure was used. Two custom sensors were immersed in a bucket of “room temperature” water. The temperature of the water was also recorded by one of the unmodified HOBO TMC-HD Air temperature sensors. The sensors were allowed to record at 1 minute intervals for a minimum of 1 hour and the results compared. All of the modified sensors recorded temperatures within ±1.0 °C of each other and the TMC-HD sensor, which determined to be within the acceptable accuracy range.

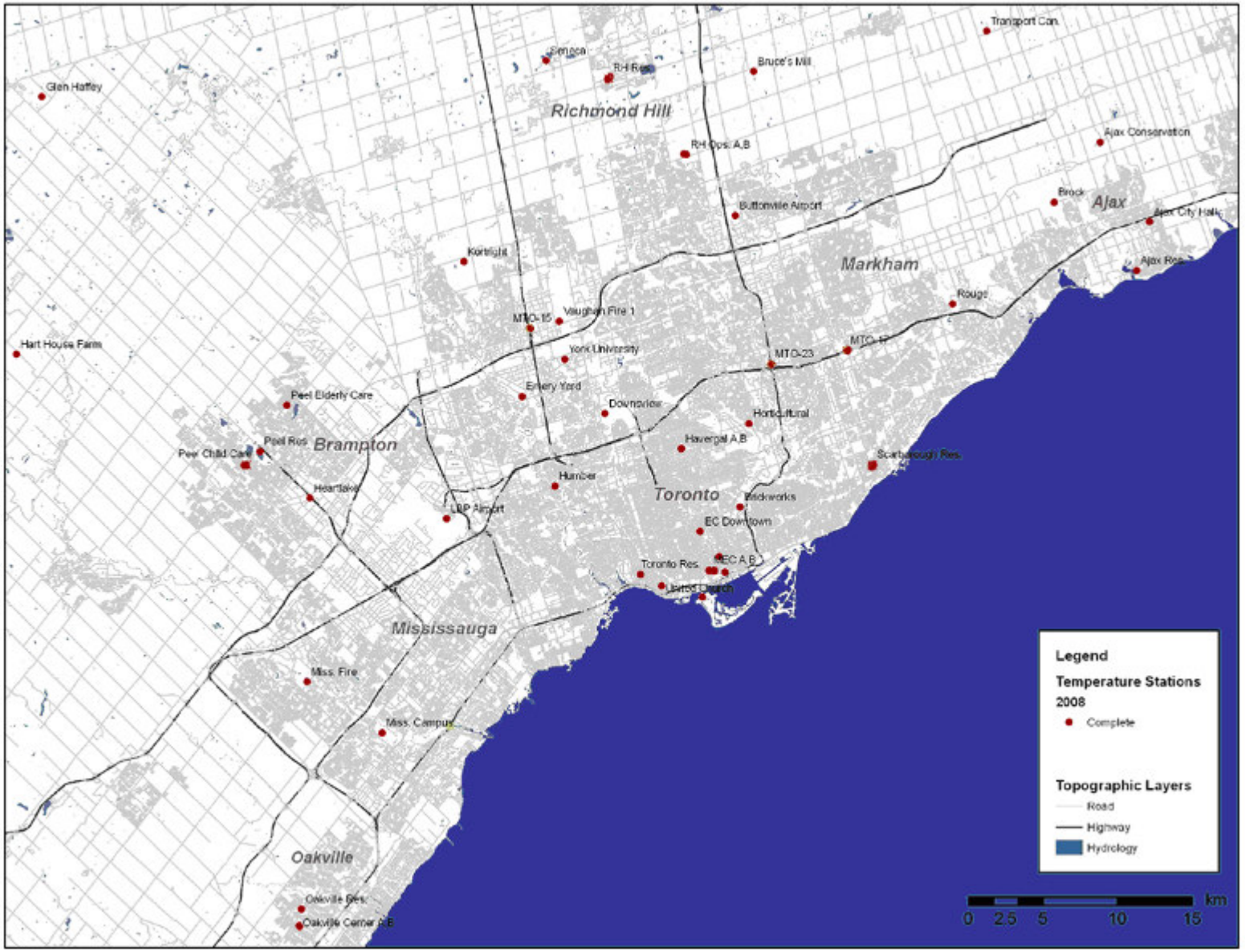

Figure 1. Study area with temperature measurement site locations.

Figure 2a. NRCan TMC-HD Air Temperature Sensor (1.5 meter mast, radiation shield).

Figure 2b. NRCan Custom Surface Temperature Sensor (secured to surface with silicone gel).

3.3. Remotely Sensed Surface Temperature Measurements

3.3.1. Acquisition

A total of 13 Landsat images from scene path 18, row 30, which covers the GTA and rural surrounds (Figure 3), were acquired. The eastern portion of the GTA, including most of Ajax is not acquired in this scene. Table 1 lists the acquisition dates and meteorological conditions for the imagery.

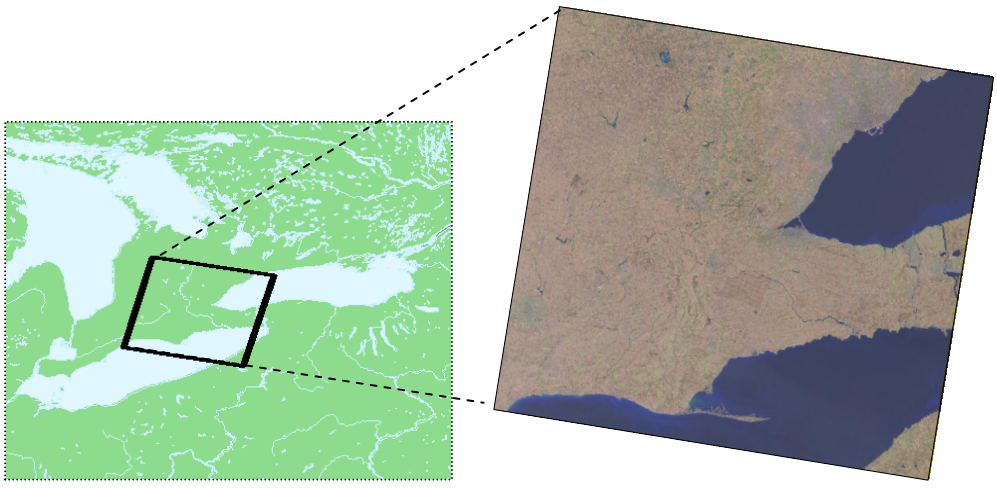

Figure 3. Southern Ontario with Landsat image (path 18, row 30) covering GTA study area.

Image Date	Sensor	Air Temp (°C)	Rel Hum (%)	Wind (km/h)
May 5, 1987	TM	15.3	31	15
Sep 2, 1990	TM	24.8	52	19
Jul 11, 1994	TM	21.1	36	9
Jul 17, 1997	TM	18.2	51	22
Sep 03, 1999	ETM	25.9	46	4
Jun 7, 2001	ETM	19.8	47	28
Aug 10, 2002	ETM	26.2	37	7
Jun 3, 2005	TM	20.1	60	17
Feb 21, 2007	TM	-0.5	73	6
Jun 29, 2007	TM	20.4	37	7
Aug 1, 2007	ETM	30.7	48	4
Jul 1, 2008	TM	23.1	43	15
Sep 3, 2008	TM	26.3	48	7

Table 1. Landsat imagery acquisitions, Land Surface Temperature map processing and meteorological conditions at the time of acquisition. Air temperature, relative humidity and wind speed for 10:00 Local Standard Time from Lester B. Pearson Airport meteorological station (Environment Canada).

3.3.2. Image Preprocessing

In order to estimate actual surface temperatures at specific locations or compare temperatures between images, the images needed to be geometrically corrected to a reliable source in order to minimize the positional error as much as possible. The images were corrected with 1:50000 Geobase road networks as reference using a first-order polynomial transformation with PCI Orthoengine software. A minimum registration accuracy of +/-120 m for TM and +/-60 m for ETM+ imagery was achieved using 25 ground control points for each image.

3.3.3. Land Surface Temperature Estimation

Landsat imagery was used to estimate LST by first converting the TM and ETM imagery digital numbers (sensor values scaled from 0 to 255) to radiance values by using gain and offset calibration values (included with the Landsat image products, but can also be found at the USGS website). LST was then be derived from radiance in the 10.4-12.5 µm spectrum by using an inverse of the Planck function (Schott and Volchol, 1985). This method, shown in Figure 4, has been tested in numerous studies with LST accuracies within the 2.0 °C range (Lillesand and Kiefer, 2000). No atmospheric correction was carried out due to lack of atmospheric condition data for the full range of images. This method also assumes an emissivity of 1.00 for each pixel.

Converting DN to Radiance

$$CV_R = G(CV_{DN}) + B$$

CV_R is the cell value as radiance
CV_{DN} is the cell value digital number
G is the gain
B is the bias (or offset)

Converting Radiance to LST

$$T = \frac{K_2}{\ln\left(\frac{K_1}{CV_R} + 1\right)}$$

T is degrees Kelvin
CV_R is the cell value as radiance
K_1 is 607.76 (for TM) or 666.09 (for ETM+)
K_2 is 1260.56 (for TM) or 1282.71 (for ETM+)

Figure 4. Land Surface Temperature conversion formulas.

3.3.4. Validation

In order to test the accuracy of the LST maps, estimated temperatures were compared to in situ surface temperature measurements from the monitoring network. Numerous studies have assessed the accuracy of Landsat based LST estimates using this method (Schneider and Mauser, 1996) and a rigorous validation was not deemed necessary. However, a limited test of the map accuracies would indicate that the method was implemented correctly and error ranges from previous studies were applicable.

Surface temperatures were collected at 10 monitoring sites on various urban surface covers throughout the study area on the dates coincidental with the 2008 imagery. The LST maps derived from July 1, 2008 and September 3, 2008 were selected for assessment. In situ measurements from 10:00 on the acquisition dates were selected as ground truth. Although none of the in situ sensors were measuring entirely homogeneous 60 or 120m surfaces to match the satellite based minimum mapping units of 1 satellite pixel, they were installed on surface covers representative of the dominant cover of city blocks or neighbourhoods. In some cases, multiple sensors were used at the same site to assess heterogeneity in surface temperatures. Table 2 shows a sample of the measurement sites and lists the in situ and collocated Landsat estimated surface temperature. Although some LST estimates differ from the in situ measurements as much as 6°C, the average difference is approximately 2.5°C. There appears to be no

systematic bias of the LST estimates and it is possible that the differences are a result of insufficient coverage by the in situ sensors to account for 60-120m pixels. For example, at the Oakville Recreation Centre monitoring site, the municipal building covers roughly 30m x 30m but is surrounded by an extensive grass recreation area. Based on these results, which support previously demonstrated accuracies of approximately 2.0°C, the LST maps are deemed accurate to within that range.

Measurement Site Location	Surface Description	In situ Surface (°C)	Landsat LST (°C)	Difference (°C)
Ajax City Hall	gravel roof	28.84	26.22	2.62
Ajax Rec. Park	grass	26.80	26.19	0.61
Oakville Rec.Centre	aluminum roof	33.59	27.25	6.34
Toronto City	gravel roof	21.50	26.19	4.95
Toronto Metro Hall	large stone roof	18.54	21.98	-3.44
Toronto CAP Office	large stone roof	23.63	24.24	-0.61
Toronto MEC Store	green roof	24.04	27.56	-3.52
Toronto Industrial	aluminum roof	34.01	36.20	-2.19
Horticultural Center	green roof	23.25	26.74	-3.48
Vaughan Fire Station	gravel roof	31.53	31.04	0.49

Table 2. In situ surface temperature sites with sensor temperatures and Landsat LST measurements from July 1, 2008.

3.3.5. Calibrated Land Surface Temperatures

As LST estimates are determined by the radiative conditions at a specific time of day and day of year, it is often difficult to compare these LST from one image date to another as the conditions are likely different. All of the images used in this study were selected for having clear sky, high-heat conditions with summer phenological conditions (i.e. leaf on) at 10:00 local time. In most cases the climatic conditions remained constant throughout the day. Despite these similar conditions there were still significant radiative and subsequent surface and air temperature differences for each day. If these differences were not too severe, the imagery should be suitable for calibration to represent relative heat event conditions. This process also assumes that there are no differences in the phenology of the crop cover in the rural surrounds of the GTA between images, which is likely erroneous. The thermal admittance differences for bare fields and crops at peak growth are an accepted error for this calibration process. However, the thermal properties of impervious covers are static throughout the summer and are still significantly different than crop cover at any stage of growth. In order to derive relative LST values for multi-temporal comparisons a series of calibrations were carried out using linear regressions.

3.4. Urban Land Cover Mapping

In order to investigate the relationships between urban surface cover and surface temperature, land cover maps were produced for the study area using imagery from 1990 and 2008. The two different land cover dates would allow comparisons of the LST maps to changes in urbanization over 18 years. Employing the non-thermal bands of the Landsat imagery in a supervised Maximum Likelihood Classifier (MLC), maps were created with 6 land cover classes (water, grass/unimproved pasture, agriculture, forested, light urban, heavy urban). The MLC is based on a probabilistic approach calculated from inputs for discrete classes established from training pixels. Each image pixel's brightness or reflectance values are used to determine membership in each class. A separate set of training data was used for the 1990 and 2008 classifications. A small portion (15%) of the training data was withheld and used to validate the classifications. The non-thermal Landsat bands were also tested against the thermal bands to assess the correlation. It was determined that the visible and NIR bands were spectrally independent of the thermal. Therefore the land cover maps and LST maps are independent and suitable for comparison.

Previous studies have explored the relationship between heat signatures and impervious surfaces. Many studies have found high surface temperatures to be correlated with significant cover of impervious surfaces (Lo et al., 1997). It is expected that areas that have changed from non-urban to urban will be related to an increased thermal response in heat event conditions.

4. Results

4.1. Air – Surface Temperature Relationships

Solar loading is the dominant control for near-surface air temperatures, however the relationship between surface and air temperatures is still difficult to characterize. When interpreting the air temperature values for a given day, the wind speed, humidity and cloud cover need to be considered. For the purposes of this study, the focus was on typical "heat event" conditions, specifically isolating low wind and low cloud cover days for analysis. Previous studies have shown that the heat island effect is most pronounced under these conditions (i.e. Oke, 1982). Results from the collocated in situ surface and near-surface air temperature measurements emphasized the indirect relationship between the two parameters under heat event conditions. Figure 5a-b shows air and surface temperatures for two 2008 summer dates from 4 GTA sites, each selected as

representative of a land use type. June 6 was clear skied with low winds (max speed < 30 km/h) and July 9 was clear skied but with relatively high winds (max speed > 30 km/h). Relationships are different for each measurement site, with Emery Yard (industrial area) and Oakville Recreation Center (dense suburban) showing significant increases in surface temperatures throughout the day but comparatively weak increases in air temperatures. In contrast, we see modest surface temperature increase at the Ajax Recreational Park and Horticultural Center (green roof) followed by a more linear increase in air temperatures. The influence of greater turbulent flux (July 9) shows closer air – surface temperature relationships, and greater similarity in temperatures between sites, likely due to increased mixing of air masses.

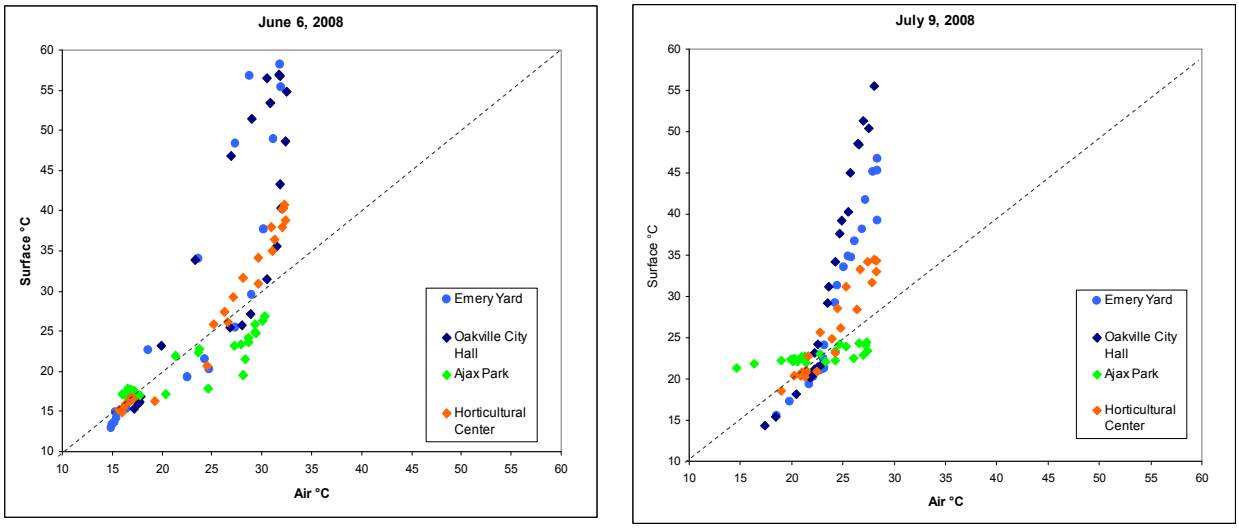

Figure 5a-b. Surface and air temperatures for 4 different GTA measurement sites on June 6 and July 9, 2008.

The observations that supported the assumption of common solar loading across the study area, were the similarities between surface temperatures on common surfaces regardless of location. This was particularly evident in the surface temperatures for non-residential structures with gravel or rock rooftops. The plotted hourly measurements for August 13th (Figure 6a), show very similar temperature responses to solar radiation among the similar surfaced roofs. Despite the large range in diurnal surface temperatures (30 °C), differences between sites rarely exceeded 5°C at any given time. This is particularly informative given that these measurement sites are up to 50 km apart. Similar results were found for other common urban cover types. Among three grass cover sites (Peel Residential, Oakville Residential and Ajax Park) and three asphalt sites (Union Station, Mississauga Fire Station, Peel Elderly Care Centre), the inter-site correlations amongst common cover types were high ($r^2 > 0.95$). These results suggest that known surface temperatures can be modeled based on cover type, as was done with the thermal imagery calibrations.

In contrast, the air temperatures for the same date over these common surfaces varied significantly (Figure 6b), with diurnal ranges of only 10°C yet up to 4°C differences between sites. The air temperatures for grass covered sites had similar diurnal ranges to the other urban covers however the grass cover site differences were less than 2.5°C. These results support those shown in Figure 9a-b, demonstrating that vegetated covers approach linear air to surface temperature relationships, whereas urban covers are less predictable. Based on this, remotely sensed surface temperatures could be used for estimating air temperatures for vegetated areas, however there would be considerable uncertainties for urban areas. These observed limitations, also question the suitability of remotely sensed surface temperatures, no matter how spatially extensive, to support air temperature modelling. Recent thermal remote sensing studies (i.e. Voogt and Oke, 2003) also address these concerns for effective UHI mapping.

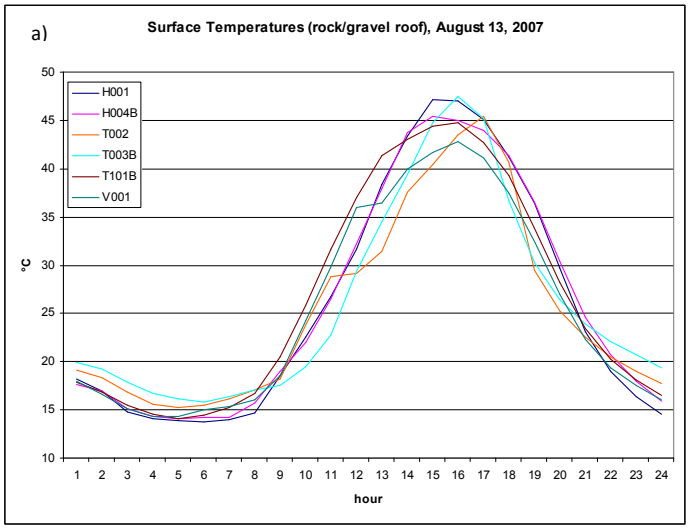

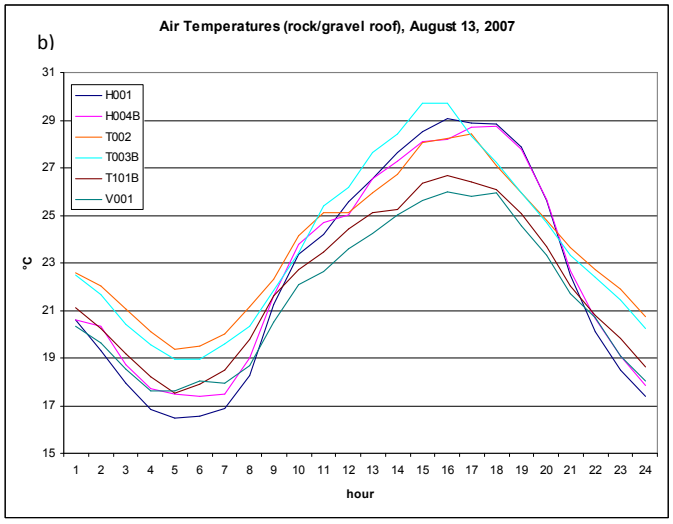

Figure 6a-b. Gravel and rock covered roof surface temperatures (a) and air temperatures (b) measured on August 13, 2007.

4.1.1. Green Roofs

This study also presented an opportunity to compare air and surface temperatures on two “green roofs” in relation to adjacent asphalt roofs. The Mountain Equipment Co-op (MEC) building in Toronto had a portion of the asphalt roof covered with grasses and sedums, seen in Figure 7a-b, with the uncovered portion as the control site. The Toronto Horticultural Center had various grasses on as covers. The Havergal College site, (1.2 km west) was used as an asphalt control for the Horticultural Center. Surface and air hourly temperatures were compared from various heat event condition days in 2007 and 2008 with results for June 26-27, 2008 at the MEC site plotted in Figure 8. The drastic differences in surface temperatures between the two roof covers are apparent, with an average difference of 9°C. However, the effect on air temperatures at 1.2 m for both roofs, is considerably smaller, an average difference of only 0.57 °C. Similar results for the Horticultural center and Havergal college sites are shown in Figure 9. Both the sites are located in the Don River Valley with substantially more surrounding vegetation than the downtown MEC site, which is the likely cause of the lower surface and air temperatures. However, again we see significant differences in surface temperatures but similar air temperatures. Another observation of note, was that the asphalt surfaces with higher thermal inertia, cool as quickly as they heat up and actually become cooler than the green roofs after 21:00 local time.

Both sets of results are typical of high heat, low wind and cloud cover days and suggest a lack of cooling effect expected from green roofs. However, the scale of these surfaces is relevant to the surface-air temperature discussion. A single 10,000 square foot green roof surrounded by asphalt and concrete surfaces several orders of magnitude larger will ultimately have little affect on air temperature, as observed at 1.2 m above the roof surfaces. It should also be noted that neither of these roofs show a cooling effect on the LST pixels. These results are far from conclusive, however they suggest more testing is required.

Figure 7a. MEC Asphalt Tile Roof

b. MEC Green Roof

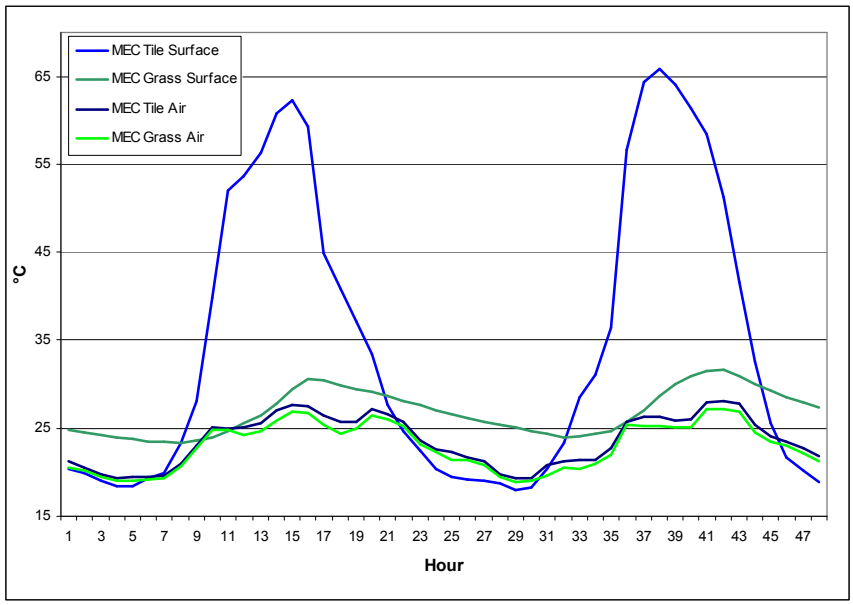

Figure 8. MEC Green roof and asphalt tile roof air and surface temperature measurements for June 26-27 2008.

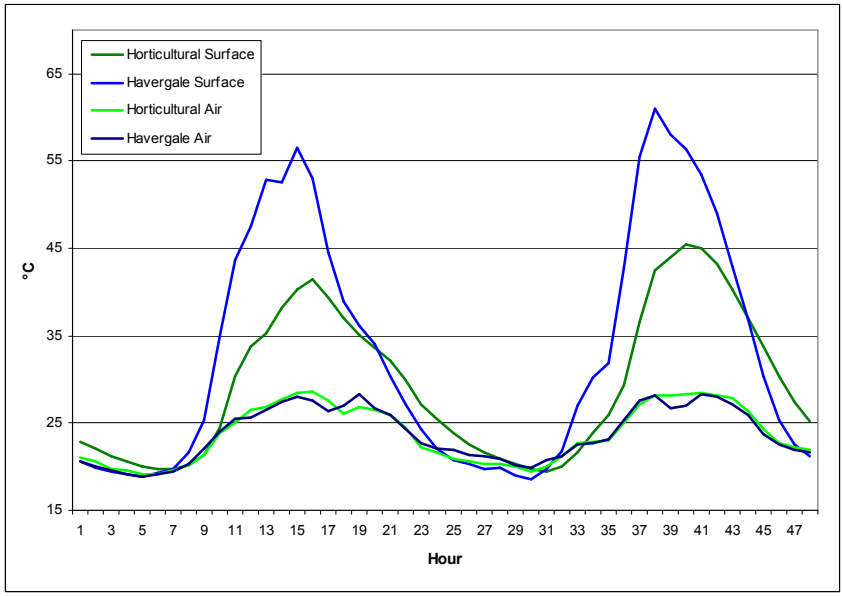

Figure 9. Horticultural Center and Havergal College Green roof and asphalt tile roof air and surface temperature measurements for June 26-27 2008.

4.2. Remotely Sensed Surface Temperatures

The production of 12 summer LST maps, along with a series of hourly and inter-annual calibrated LST maps allowed the analysis of spatial and temporal variations across the GTA. The LST maps were deemed valid to approximately 2.5°C based on in situ measurements and previous assessments of Landsat TM and ETM+ imagery. As previously discussed, there are some inherent difficulties in deriving air temperatures from surface temperature measurements, however a positive relationship does exist between the two variables and the maps are still considered informative to understanding UHI extents and intensities.

4.2.1. Surface Urban Heat Island

The 2002 LST image in Figure 10 shows the typical 10:00 local time thermal regime for heat event conditions. There are clear surface temperature differences between urban and rural areas, typically between 5 and 10 °C. It should be noted that there is significant variation in rural surface temperatures, likely due to albedo differences from bare fields and various stages of crop development. Another observation that requires consideration is that the downtown core has lower surface temperatures than much of the peripheral suburban and urban cover. Figure 11 shows higher resolution subsets of suburban Brampton and the downtown Toronto core. With perhaps the greatest amount of impervious cover and highest density of multi-storey structures, one would expect the core to have the highest surface temperatures. However, the suburban cover appears to have distinctly higher thermal admittance properties. One possible explanation is the shading effects from the high buildings is likely affecting the LST estimates. There may be other factors affecting the actual surface temperatures, such as winds from Lake Ontario influencing sensible heat fluxes. The lowest surface temperatures within the urban fringes are found in the vegetated corridors such as the Don and Humber river valleys. This study lacked extensive in situ measurements within these corridors to assess whether the lower surface temperatures from vegetation cover translate into cooler air temperatures.

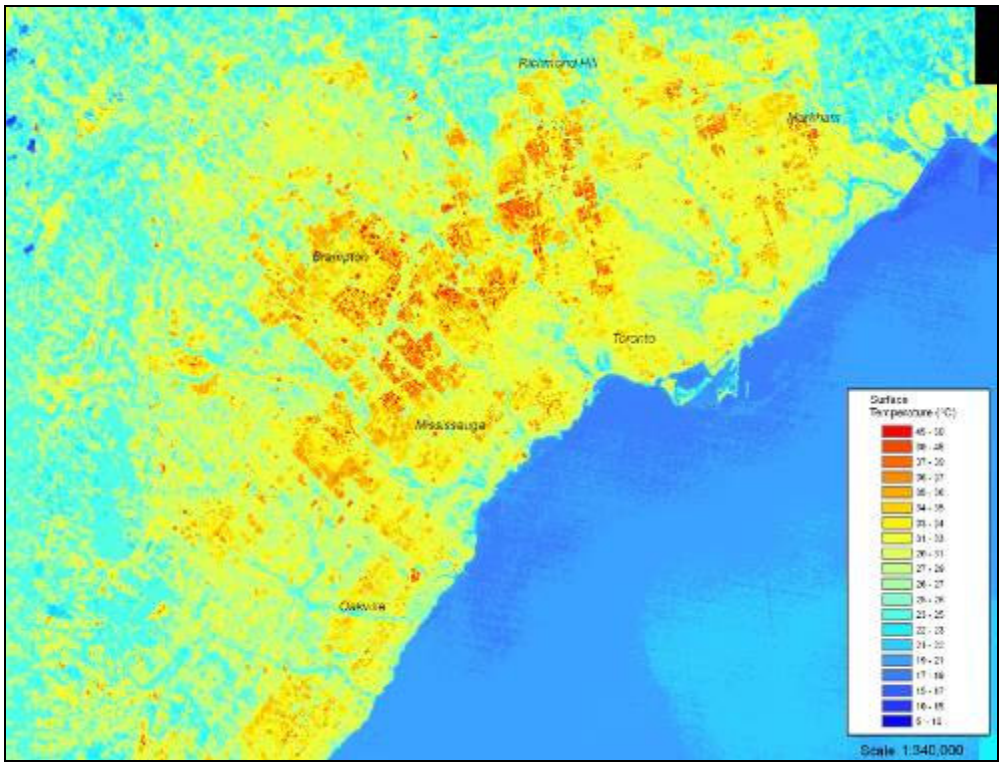

Figure 10. Land Surface Temperature Map of the GTA August 10, 2002

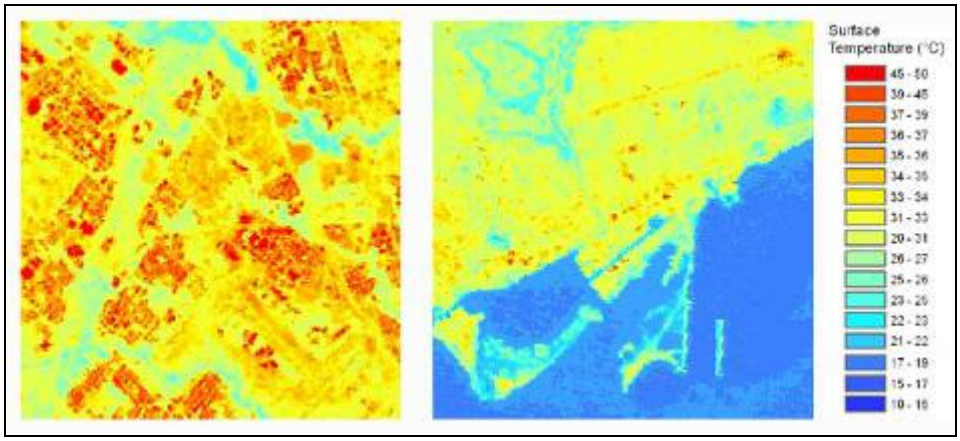

Figure 11. a)Suburban (Brampton) and b) Urban (Downtown Toronto) subsets of August 10, 2002 Land Surface Temperature map.

4.2.2. Calibrated Land Surface Temperatures - Diurnal

Access to both point diurnal surface temperatures from a wide range of urban covers and spatially extensive single-time (10:00) Landsat derived surface temperatures, presented some interesting calibration opportunities. When plotting the 10:00 in situ surface temperatures against surface temperatures from other times of day, distinct linear relationships were present (Figure 12). As expected, in cloud free conditions, common covers have similar thermal responses to solar radiation. Based on these temporal relationships, it was deemed possible to calibrate the LST maps to visualize the diurnal surface temperature variations across the GTA. The 50 surface temperature sites were not representative of all cover types in the GTA, particularly omitting natural corridors and some of the industrial areas. However, the surface measurements did represent many of the dominant cover types, particularly those of commercial multi-storey structures, suburban homes and rural areas. Given the LST validation results (2.0 °C) and the variability in the multi-temporal relationships, the calibrated products are not likely to offer accurate diurnal point surface temperatures, however they give insight into the spatial patterns of surface heating and cooling. The July 1, 2008 image was selected for calibration due to its low cloud cover and typical "hot-day" conditions. Figure 13 shows the original 10:00 LST map as well as the calibrated LST maps for 14:00, 18:00 and 24:00 respectively.

These diurnal calibration results are informative to the GTA surface heat island allowing temporally and spatially explicit visualizations of the surface thermal regime. From 10:00 to 14:00 there is considerable heating among urban surfaces (10 °C), however through 18:00 and onto midnight, there is uniform cooling among all surfaces.

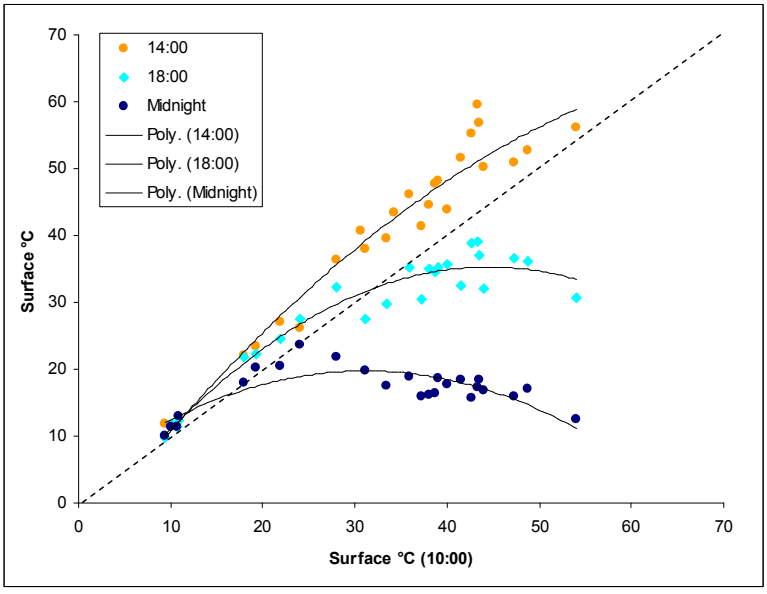

Figure 12. July 1, 2008 in situ surface temperature (50 sites) plotted for 10:00 against 14:00, 18:00 and 24:00.

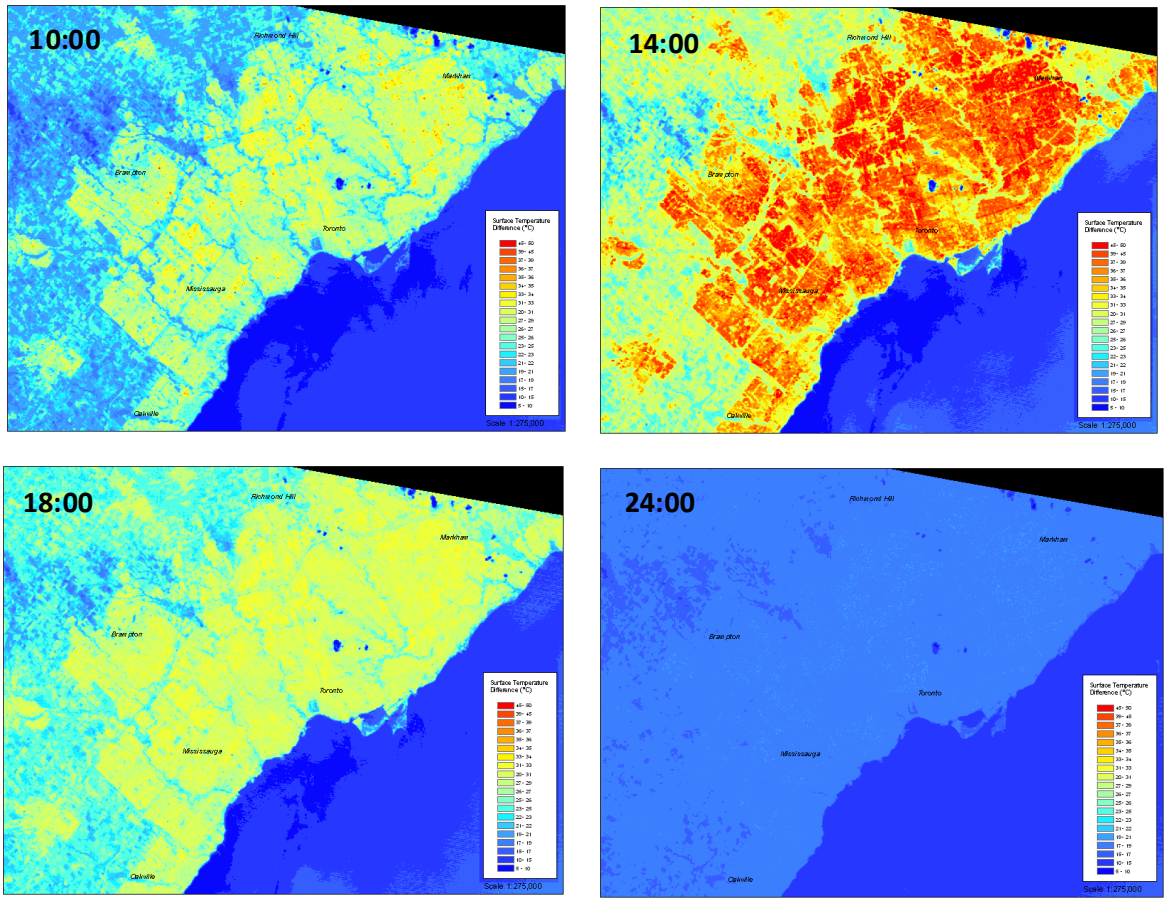

Figure 13. July 1, 2008 LST maps for 10:00 and calibrated to 14:00, 18:00 and 24:00.

4.2.3. Flux Footprint and Air Temperature

The in situ air temperature measurements suggest that there is little difference in air temperature between proximal sites despite different surface covers and subsequent surface temperatures (i.e. MEC green roof in downtown Toronto). This suggests that air temperature at 1.5m is determined by heating from surfaces of source areas (or flux footprints) that are larger than a standard rooftop. Although most of the in situ measurements were placed on representative surface covers, it was rare that they could encompass the wide range of covers in a typical city block (i.e. lawns, roads, roofing).

Initial research on flux footprints (Schmid 2002; Leclerc et al., 1990), demonstrates that most of the heat flux contribution at 1 m heights typically comes, from not just immediate surface, but from several hundreds of meters of surface downwind of the measurement. In order to test the impact of the flux footprint on the surface air temperature relationship, the LST pixels downwind of each monitoring site were

averaged from distances of 240m, 360m, 600m and 900m and correlated with the 1.5m air temperatures. Figure 14 shows these correlations between flux footprint LST and air temperature for July 1, 2008 (280° wind direction) and August 1, 2007 (160° wind direction). It is initially surprising to see how low the typical LST to air temperature correlations are, particularly for the 10:00 values (r^2 = 0.13), which correspond to the LST estimate times. As footprint size increases from 120m to roughly 600m LST to air temperature correlations increase. The midnight temperatures had the highest correlations, with up to 0.75 values for 480m footprints. These results reinforce the notion that the air temperature in urban environments is largely determined by the surface properties of over several hundreds of meters as oppose to those of the immediate surface. The fact that the relationships between surface and air temperature improve as the day progresses also demonstrates the gradual response of air temperature to surface heating.

These results poses some contradiction towards common remote sensing ideologies, which tends to seek higher resolution of the measurements and suggests that relationships between physical processes deteriorate as both distance and time from the observation increase. According to the two image dates tested, the optimal resolution for determining air temperature may not be 120m but instead a value averaged over a larger area. The temporal correlation results also suggest an air temperature lag effect, such that under certain climatic scenarios (heat event conditions with no changes in cloud cover or winds), that 10:00 LST are appropriate for estimating nighttime air temperatures. It should also be noted that the flux footprint results suggest the required surface area (480m) to create a heat island that would be felt at 1.5m height.

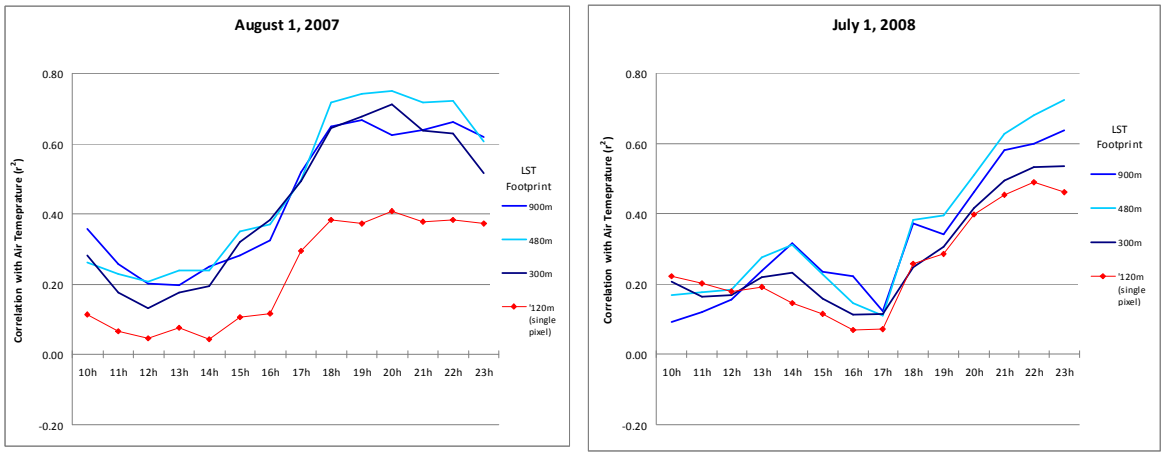

Figure 14. 10:00 Land Surface Temperature and Hourly Air Temperature correlations for various footprints (downwind pixels) for August 1, 2007 and July 1, 2008.

4.2.4. Surface Temperature Change 1990-2008

In order to determine relative temperature changes for the 1990 to 2008 time period, a series of images were calibrated by linear regression to match the conditions of the August 10, 2002 image. This image was selected as the baseline for three reasons; the image was an ETM+ image capable of calibrating both 60-120 m pixels, the atmospheric conditions were ideal with minimal water vapour and high visibility and the image represented a typical high heat, low humidity day with no recent rain events prior to the acquisition. Archived meteorological data from the Lester B. Pearson Airport lists the air temperature at 26.2 °C, the humidity at 35% and the wind speed at 7km/h at the time of image acquisition.

The calibration was carried out by first selecting sites over a full range of land covers which remained unchanged for the entire range of imagery dates (1987-2008). Water temperatures, particularly those of Lake Ontario have been ignored as they respond much slower to solar radiation than those of land surfaces. The sites also needed to cover areas that would be relatively homogeneous under 120 m pixels. Based on interpretation of recent and archived air photos, 96 calibration sites were selected as shown in Figure 15.

Figure 15. Calibration sites (red points) displayed over August, 10, 2002 Landsat image.

Using the calibration site locations, each image was queried for LST values which were then compared to the baseline LST values from the August 2002 image, as shown in

Figures 16a-d. Using the scatter plots and r^2 correlation coefficients it was determined whether a linear regression was suitable to fit the LST values of a given image to the baseline image. In many cases, the correlations were too low with high variability, likely due to high soil moisture levels from the pervious surfaces. In other cases (i.e. September 3, 1999) no calibration was required as the climate conditions were very similar to those of the baseline image. Based on this method, four LST maps were calibrated for multi-temporal comparison with the August 10, 2002 LST map.

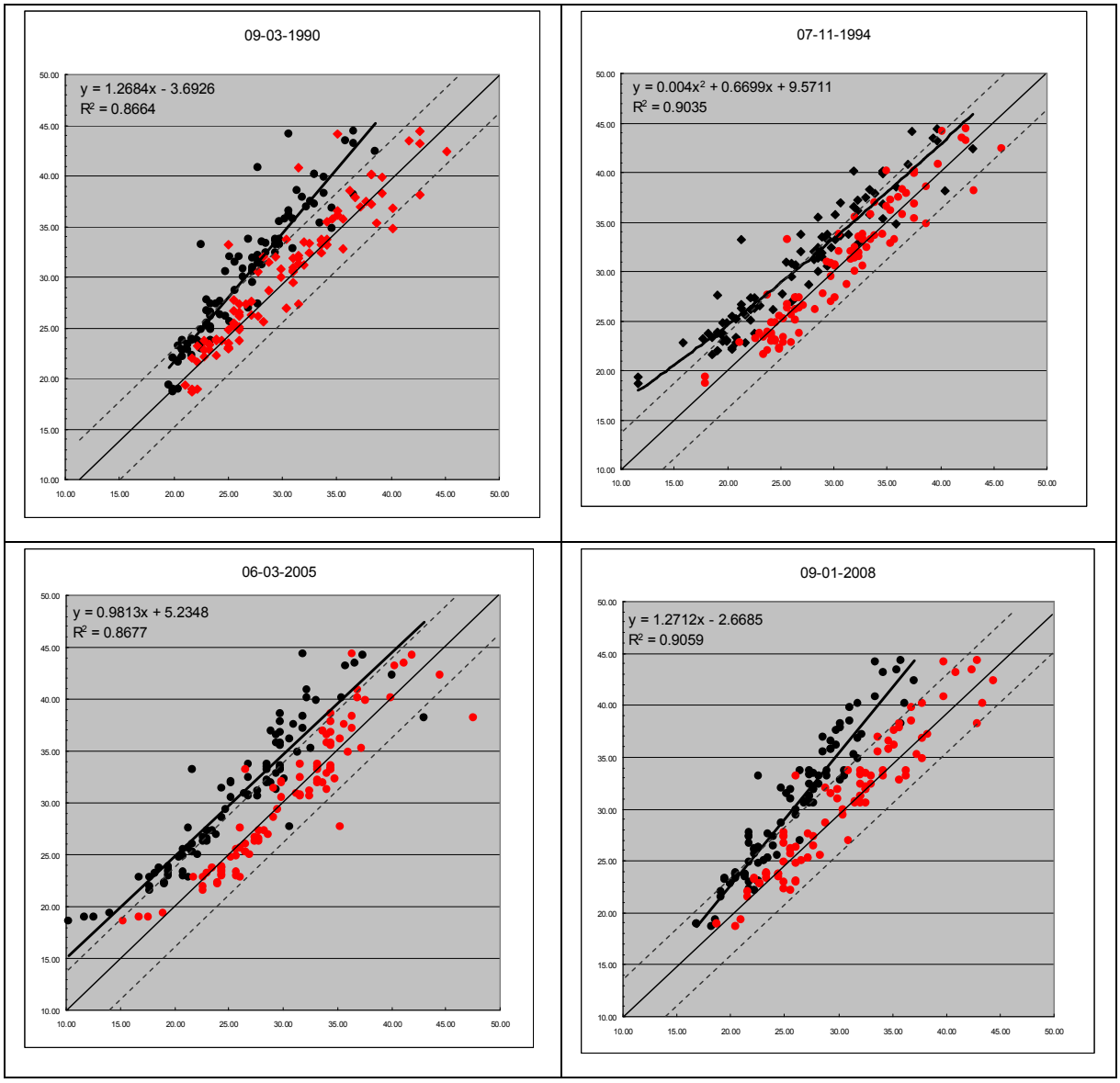

Figure 16a-d. Individual (y-axis) and August 10, 2002 baseline (x-axis) surface temperatures plotted in black with r^2 values. Calibrated and baseline imagery surface temperatures plotted in red.

Figure 17 shows a differenced image of the calibrated 1990 and 2008 LST maps giving an indication of areas that had undergone significant changes in thermal properties, specifically how they respond to a typical summer heat event day. The urban core and rural peripheries show little heating or cooling differences from the calibrated 1990 and 2008 maps. However the suburban fringes, the location of new housing developments found in Brampton, Richmond Hill, Mississauga and Oakville show between 5 and 15 °C temperature increases.

When compared to the 1990 to 2008 land cover change map, Figure 18, there is a close relation between temperature increase and new urban development. As one would expect, replacing vegetated covers with roadways and urban structures will have a dramatic effect on the surface's ability to absorb solar energy. Further comparisons are required to determine the extent of this relationship and if factors such as building density or building type factor into increases in surface temperatures in heat event conditions.

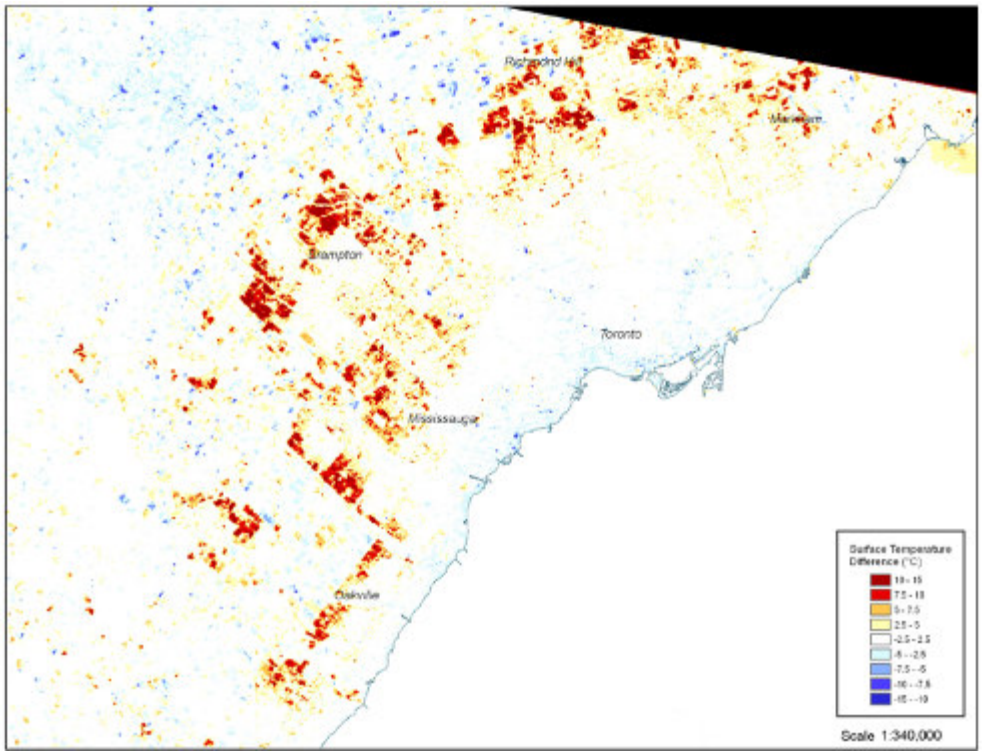

Figure 17. Relative Land Surface Temperature change 1990 -2008. Lake Ontario delineated for reference.

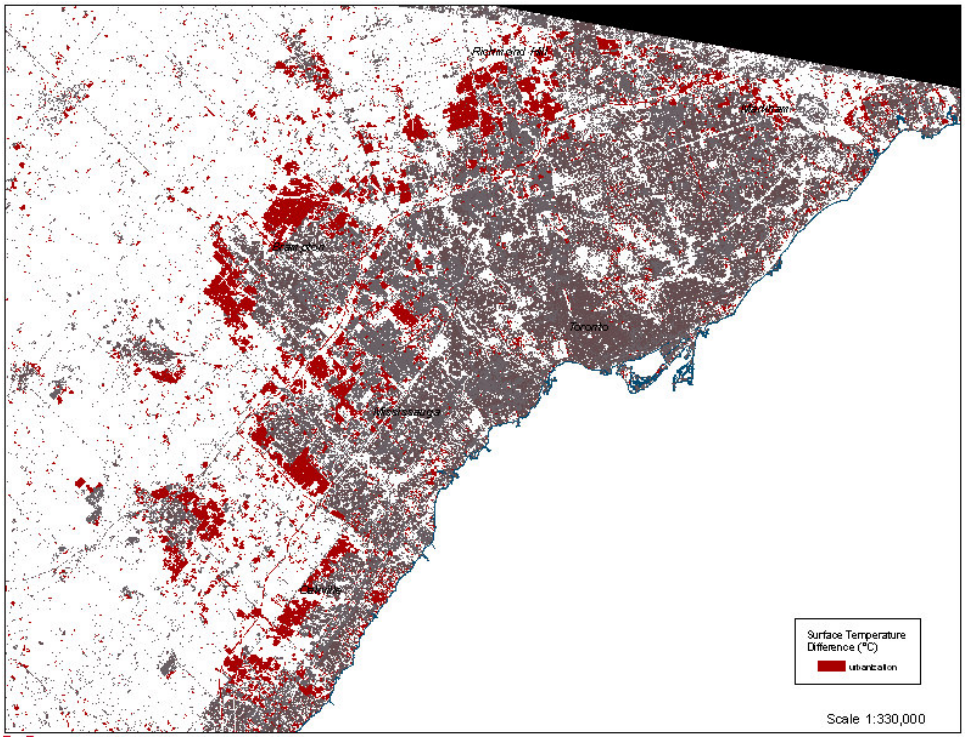

Figure 18. Urban Land Cover change 1990 - 2008, grey areas indicating urban cover in both 1990 and 2008, red areas indicating change from non-urban in 1990 to urban class in 2008.

4.3. Spatial and Temporal Heat Variations in the Greater Toronto Area

The in situ and remote sensing temperature measurements present an opportunity to characterize the surface and canopy layer UHI of the GTA. The absence of extensive wind flux and radiation measurements prevent any spatially explicit modelling, however some spatial and temporal relationships are particularly informative.

The in situ air and temperature measurements suggest several microclimates or heat islands within the GTA, however when the results are averaged by land use class across the study area, a generalized air temperature UHI trend is evident. Seven rural sites (Bruce Mill, Glen Haffey, Goodwood, Heartlake, Kortright, Seneca, Transport Canada), seven urban sites (United Church, CAP Office, Metro Hall A, Union Station, MEC A, Brickworks, Emery Yard) and seven suburban (Ajax City Hall, Ajax Residential, Oakville Center, Oakville Residential, Peel Residential, RH Residential, Mississauga Fire) sites were used in the analysis. Although other additional site measurements were available, it was decided to use the same number of sites per land use class as well as to omit anomalous

measurements (i.e. green roofs). Inter-land use class temperature variability was considered to be quite low (mean standard deviations < 1.20) therefore permitting class aggregations across the GTA. As with previous UHI studies, the rural sites are assumed to be the control, on which the urban and suburban sites will be assessed.

Figure 19 shows hourly air temperature values for July 1, 2008 averaged by land use class. These results present a weak daytime UHI, with less than 1.75°C differences between urban and rural sites from 8:00 until 20:00. However, the suburban sites have a slight daytime UHI when compared to the rural areas. Both urban and suburban sites have a pronounced nighttime UHI, with 1.92-5.26°C intensities, when compared to rural sites. To test the persistence of the day and nighttime UHI for the GTA, the average noon and midnight air temperature land use class were compared for each day over the month of August 2008. A clear and consistent nighttime UHI effect is present, with a negligible daytime effect as seen in Figures 20 and 21. A t-test was used to determine if temperatures were significantly different between land use classes ($p>0.05$). T-tests revealed no significant differences between the August noon air temperatures for the urban, suburban and rural classes. However, the midnight air temperatures were deemed significantly different for the each of the urban, suburban and rural classes.

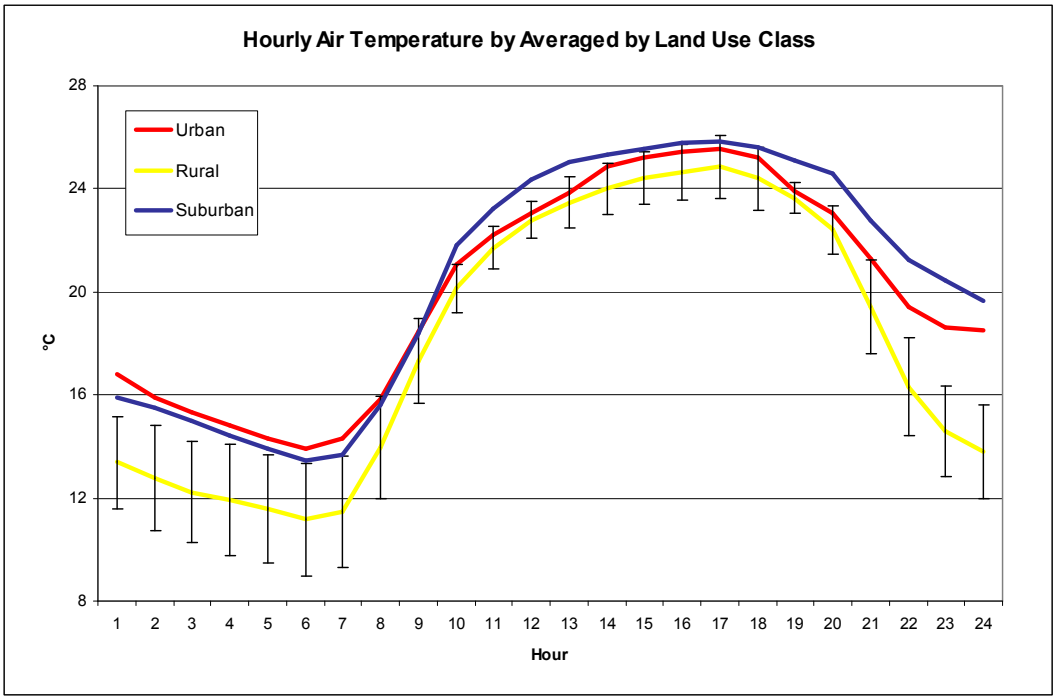

Figure 19. Hourly air temperature values for July 1, 2008 averaged by urban, rural and suburban classes. Error bars for rural standard deviations plotted.

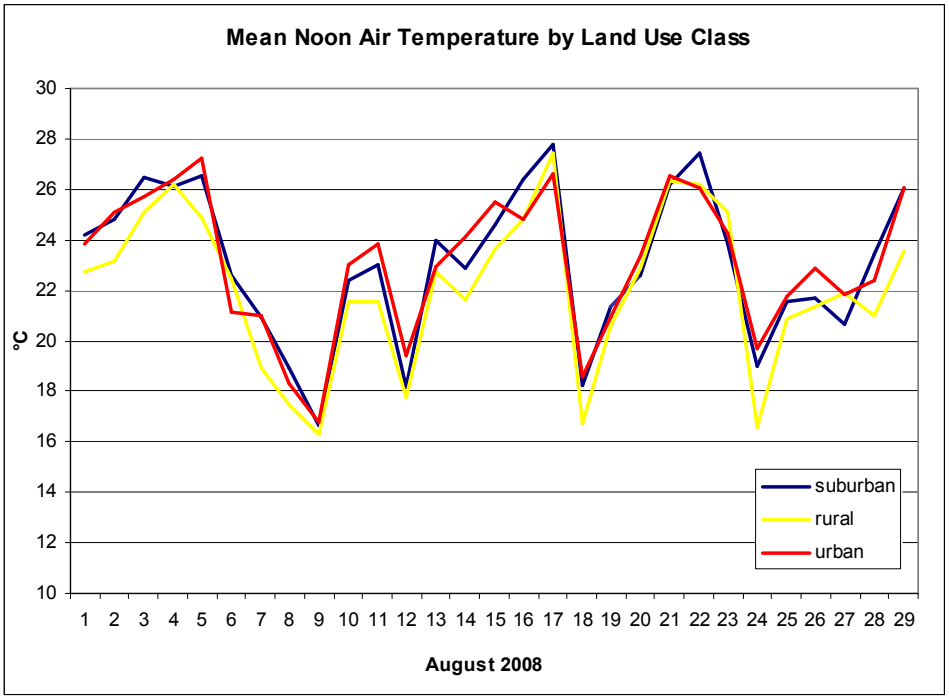

Figure 20. Noon air temperature values for August, 2008 averaged by urban, rural and suburban classes.

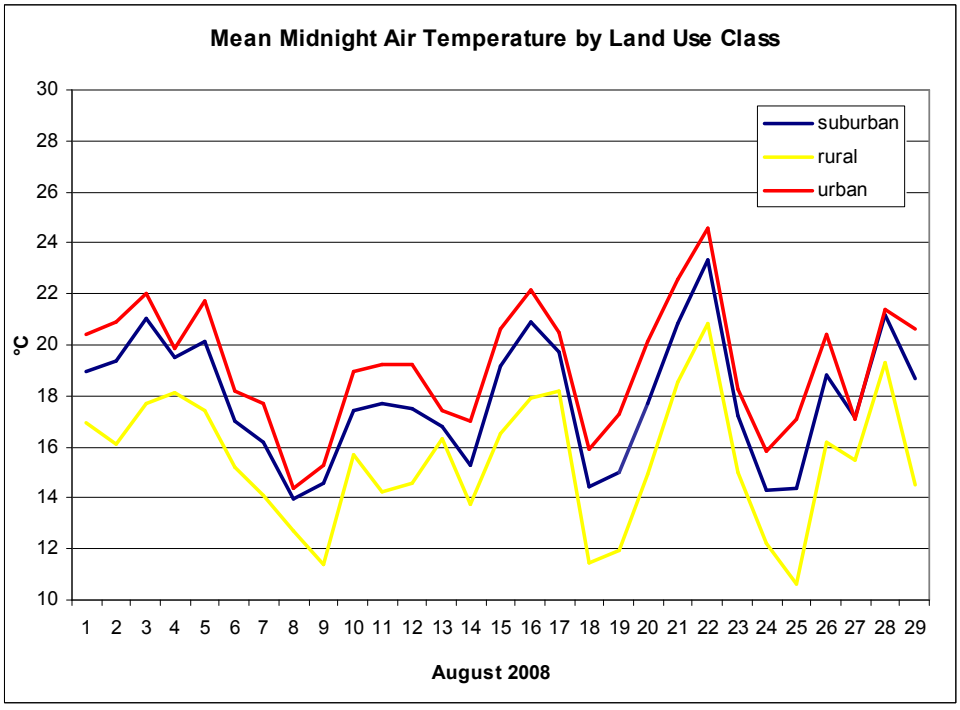

Figure 21. Midnight air temperature values for August, 2008 averaged by urban, rural and suburban classes.

While the air temperature measurements show a modest daytime UHI, the surface temperature measurements show different diurnal heat island patterns. The LST maps demonstrate a dramatic daytime surface heat island (i.e. Figure 14) with greater than 15 °C differences between urban and rural areas, however the nighttime in situ and calibrated surface temperatures (i.e. Figure 6) show an absence of a nighttime surface heat island. While the results may appear contradictory, they support the "urban canyon" concept of Oke (1987). Although the urban surfaces may have released the heat that was admitted during peak solar hours, the heated air is still trapped in urban canyons. While the rooftops may cool rather quickly, the walls and canyon surfaces may be trapping and re-emitting long-wave radiation.

Based on the above mentioned discrepancies, the remote sensing technologies (i.e. Landsat) used in this study are limited in their ability to characterize the thermal properties of the urban canyon. However, the daytime surface heat islands and nighttime air heat islands are strikingly similar and provide accurate spatial estimates of the solar loading, which is the dominant control for air temperatures. As shown in the discussion on flux footprints the LST measurements, remotely sensed surface temperatures can be related to air temperatures at coarse scales (600m). Morning LST measurements have also been correlated to nighttime air temperatures at up to r^2 of 0.70, suggesting the 10:00 Landsat LST maps are representative of air temperature hot/cool spots, although lacking spatial and temporal accuracy.

These relationships are still tenuous and not sufficient for prediction as they are not informative in terms of urban canyons and how the density and geometry of urban structures trap heat. Recent research has focussed on urban canyon geometries as well as the surface thermal properties in UHI models (i.e. Grimmond and Oke, 1999).

4.3.1. Regional Heat Islands

The GTA heat island morphology is defined not only by the Toronto central business district, but also the suburban areas which can exhibit the highest daytime surface temperatures and nighttime air temperatures. The thermal regimes of Toronto, Brampton, Oakville and Ajax were investigated.

Three heat event days, with conditions typical for urban heat island formation, were considered for the analysis (June 8, 2008; July 1, 2008; July 7, 2008). The mean and standard deviation for air temperatures for noon and midnight for each region are shown in table 2. The Toronto site air temperatures are some of the hottest and coolest within the GTA, with numerous land use types and structural heterogeneity leading to variation across the region. Ajax sites have the coolest temperatures of the regions compared, however this is likely due to the inclusion of two TRCA sites located in parks. The Oakville

region sites had the hottest air temperatures, although a bias is suspected as no Oakville sites were located in parks. Finally, the Brampton sites which had a good mix of land use classes, had marginally higher air temperatures than the Toronto region sites. These results suggest that the suburban dominated peripheral regions may act as localized heat islands with the central Toronto region a much more complex microclimatology.

	Noon		Midnight	
	Mean	σ	Mean	σ
Ajax	25.51	2.19	22.21	1.61
Brampton	30.54	0.56	26.06	0.64
Oakville	32.15	1.10	26.76	1.05
Toronto	28.87	2.56	24.15	1.56

Table 2. Mean and Standard Deviation air temperatures by region for June 8, 2008; July 1, 2008; July 7, 2008.

5. Conclusions and Recommendations

The thermal landscape of the GTA was characterized through an extensive set of in situ measurements and coarse scale thermal images. The research focused on the spatial and temporal patterns of urban heat but also tested the suitability of remote sensing for characterizing North American UHIs.

This study first determined the validity of LST estimates from Landsat TM and ETM+ imagery. Based on in situ surface temperature measurements on a variety of urban covers, it was determined that LST estimates were approximately +-2.5°C. The LST maps were deemed suitable for coarse scale (neighborhood) analysis of surface heating.

Comparisons of in situ surface temperature results across the study area showed similar diurnal variations for common surface covers (i.e. asphalt, grass, stone). Based on these in situ results it was deemed possible to predict surface temperatures at different times of day from a single measurement. The Landsat 10:00 LST estimates were then calibrated to visualize the spatial variations of surface temperatures across the GTA at different times of day.

The relationships between surface and near-surface air temperatures was thoroughly explored to assess the potential for heat island characterization with the LST measurements alone. Surface and air temperatures across common surface covers under

typical heat event conditions were assessed. As expected, the relationships for urban covers were related but non-linear, with significant surface heating during solar noon only modestly matched by air heating.

The air and surface temperature measurements also permitted an investigation of urban heat across the GTA. The air temperature measurements from 2007 and 2008 indicated a weak daytime UHI, with little differences between urban, suburban and rural sites. However, both the urban and suburban sites had a pronounced nighttime UHI, when compared to rural sites. The reverse was true for the surface temperature measurements, with extreme temperatures differences between urban and rural areas during peak solar hours, but little difference between urban and rural during nighttime periods of cooling. It was also observed that dense suburban areas, such as Oakville, Brampton and Mississauga had the highest surface temperatures and the highest nighttime UHI intensities. These spatial and temporal variations were comparable to observations from other North American cities (i.e. Quattrochi et al., 1994; Streutker, 2002).

This study demonstrated that correlations were quite low between the satellite derived 10:00 LST and near surface air temperature suggesting thermal remote sensing may not be appropriate for UHI mapping. However, both temporal and spatial aspects of this relationship were explored. If LST pixels downwind of the air temperature measurements are averaged, the correlation improves. The 10:00 LST measurements also correlate well with nighttime air temperatures. This supports the logic that if a substantial urban area (i.e. 500m or several city blocks) did not show substantial daytime surface heating, there will not be any heat emitted and no nighttime urban heat island effect. Conversely, the observed urban and suburban areas that showed significant daytime heating, were likely to have consistent elevated air temperatures during the night.

It should also be noted that, based on the observed nighttime air heat island with a corresponding lack of surface heat island, the canyon effect may be a component of these heat fluxes. Future research on the GTA should attempt to parameterize the dense and complex arrangement of urban structures that not only absorb solar radiation but trap long wave radiation and limit air flow. The thermal imagery, despite its relatively accurate surface temperature measurements, failed to measure the walls of the urban structures, which may represent a significant portion of surface area and subsequent heat fluxes. This also may explain the differences in the observed air and surface heat islands. Voogt and Oke (2003) discuss this thermal anisotropy as a central limitation for the use of the thermal imagery.

Despite the limitations of thermal remote sensing and the observed discrepancies between surface and air temperatures, the LST maps were still found to relate to nighttime air temperatures and can still serve as indicators for urban heat island intensities. A series of images from 1990 to 2008 were calibrated to standard heat event conditions for a relative thermal change detection. The calibrated LST maps were

differenced and then compared to land cover change maps. There was a direct relationship between urbanization and substantial increases in surface temperatures in heat event conditions. There were no extensive air temperature measurements for the past 20 years in urban and rural areas to verify impact of increased solar loading.

It is hoped that the results in this study can support coarse scale analysis of urban heat in the GTA. With the increase in urbanization and projected increase in heat events due to climate warming, the LST maps can assist in understanding the impacts to human health and mitigation strategies.

6. References

Axelsson, S., Lunden, B., 1988. Atmospheric Correction of Thermal Infrared Data from LANDSAT-5 for Surface Temperature Estimation, *Proceedings of the Conference January, 1988, Spectral Signatures of Objects in Remote Sensing*.

Barsi, J.A., J.R. Schott, F.D. Palluconi, D.L. Helder, S.J. Hook, B.L. Markham, G. Chander, E.M. O'Donnell., 2003. Landsat TM and ETM+ thermal band calibration. *Canadian Journal of Remote Sensing*, 29, 2.

Fouillet A., Rey G., Laurent F., 2006. Excess mortality related to the August 2003 heat wave in France, Int Arch Occup Environ Health 80:16–24

Goetz, S. J., R. N. Halthore, F. G. Hall, B. L. Markham., 1995. Surface temperature retrieval in a temperate grassland with multi-resolution sensors. *Journal of Geophysical Research.* 100, 12.

Grimmond, C.S.B., Oke, T.R., 1999: Aerodynamic properites of urban areas derived from analysis of surface form. *J. Appl. Meteorol*. 34, 1262-1292.

Leclerc, M.Y., Thurtell, G.W., 1990, Footprint prediction of scalar fluxes using a Markovian analysis, Boundary-Layer Meteorology 52: 247-258.

Lillesand, T.M., Kiefer, R.W., 2000. *Remote Sensing and Image Analysis,* 4th Edition. John Wiley and Sons, New York

Lo, C.P., Quattrochi, D.A., Luval, J.C., 1997. Application of high-resolution thermal infrared remote sensing and GIS to assess the urban heat island effect. International Journal of Remote Sensing

Markham, B. L. and J. L. Barker., 1986. Landsat MSS and TM post-calibration dynamic rangers, exoatmospheric reflectance and at-satellite temperatures. *EOSAT Landsat Tech. Notes* (Aug.): 3-8. Natural Resources Canada, 2007. From Impacts to Adaptation: Canada in a Changing Climate 2007

Oke, T.R., 1997. Boundary Layer Climates. 2nd ed., Methuen, London Methuen: London and New York.

Oke, T. R., 1982: "The energetic basis of the urban heat island," Quarterly Journal Royal Meteorological Society, 108, 1-24.

Oke, T. R., 1981. Canyon geometry and the nocturnal heat island. Comparison of scale model and field observations, Journal of Climatology, 1, 237-254.

Peña, M.A., 2008. Relationships between remotely sensed surface parameters associated with the urban heat sink formation in Santiago, Chile. International Journal of Remote Sensing. 29: 4385 - 4404

Rosenfeld A.H., Akbari H., Bretz S., Fishman B.L., Kurn D.M., Sailor D. and Taha H. 1995. Mitigation of urban heat islands: materials, utility programs, updates. Energy and Buildings 22, 255-265.

Roth, M., Oke, T. R., Emery, W. J. 1989. Satellite-derived urban heat island from three coastal cities and the utilization of such data in urban climatology. International Journal of Remote Sensing

Schott, J. R., W. J. Volchok., 1985. Thematic Mapper thermal infrared calibration. *Photogrammetric Engineering and Remote Sensing,* 51. 9.

Schneider K., Mauser W., 1996. Processing and accuracy of Landsat Thematic Mapper data for lake surface temperature measurement. *International Journal of Remote Sensing,* 17.

Snyder, W. C., Wan, Z., Feng, Y. Z., 1998. Classification-based emissivity for land surface temperature measurement from space. *International Journal of Remote Sensing*, 19, 14.

Sobrino, J.A., Jimenez-Munoza, P., 2004. Land surface temperature retrieval from LANDSAT TM 5. *Remote Sensing of Environment,* 90.

Stroeve, J., Haefliger, M., Steffen, K., 1996. Surface temperature from ERS-1 ATSR infrared thermal satellite data in polar regions. *Journal of Applied Meteorology*, 35, 8.

Streutker, D. R. (2002). A remote sensing study of the urban heat island of Houston, Texas. International Journal of Remote Sensing, 23(13), 2595–2608

Voogt, J.A., Oke, T.R., 1998. Effects of urban surface geometry on remotely-sensed surface temperature. *International Journal of Remote Sensing*, 19, 5

Voogt, J.A. and T.R. Oke. 2003. Thermal remote sensing of urban areas. *Remote Sensing of Environment*, special issue on Urban Areas, 86(3), 370-384.

Schmid, H.P., 2002. Footprint modeling for vegetation atmosphere exchange studies: a review and perspective. Agricultural and Forest Meteorology 113, 159-183.

Appendix I – Temperature Measurement Sites

Site	Owner	Land Use Class	Measurement Surface	Longitude	Latitude
Ajax City Hall	NRCan	Urban (Municipal)	roof, stones	-79.02007	43.85075
Ajax Conservation	NRCan	Rural	grass	-79.05991	43.89948
Ajax Residential	NRCan	Suburban	grass	-79.03196	43.82161
Brickworks	NRCan	Urban (Industrial)	roof, asphalt	-79.36624	43.68423
Brock	TRCA	Rural	grass	-79.09921	43.86389
Kortright	TRCA	Rural	grass	-79.72862	43.58332
Buttonville Airport	EC	Urban (Commercial)	grass	-79.36532	43.86017
CAP Office	NRCan	Urban (Commercial)	roof, stones	-79.38450	43.65429
Emery Yard	NRCan	Urban (Industrial)	roof, aluminium	-79.54608	43.75331
Glen Haffey	TRCA	Rural	grass	-79.94292	43.93854
Goodwood	TRCA	Rural	lot, asphalt	-79.59280	43.83515
Hart House Farm	UofT	Rural	grass	-79.96703	43.78314
Havergal College	NRCan	Urban (Commercial)	roof, asphalt	-79.41437	43.72014
Heartlake Industrial	TRCA	Urban	asphalt	-79.72416	43.69405
Horticultural Center	NRCan	Urban (Green Roof)	roof, grass	-79.35767	43.73431
Humber	TRCA	Urban	grass	-79.52007	43.69886
King	TRCA	Rural	grass	-79.79275	43.84856
L.B.P. Airport	EC	Urban (Commercial)	grass	-79.61058	43.68027
MEC Asphalt	NRCan	Urban (Commercial)	roof, asphalt	-79.39305	43.64601
MEC Greenroof	NRCan	Urban (Green Roof)	roof, grass	-79.39305	43.64601
Metro Hall - North	NRCan	Urban (Commercial)	roof, stones	-79.38878	43.64570
Metro Hall - South	NRCan	Urban (Commercial)	roof, stones	-79.38878	43.64570
MTO -Vaughan	MTO	Urban (Industrial)	grass	-79.53932	43.79455
Mississauga Campus	UofT	Urban (Commercial)	grass	-79.66711	43.55176
Mississauga Fire	NRCan	Urban (Commercial)	roof, asphalt	-79.72863	43.58333
Oakville Center A	NRCan	Urban (Municipal)	roof, aluminium	-79.71714	43.48032
Oakville Center B	NRCan	Urban (Municipal)	roof, stones	-79.73865	43.43623
Oakville Residential	NRCan	Suburban	grass	-79.73639	43.44612
Peel Child Care	NRCan	Suburban	roof, stones	-79.74213	43.75029
Peel Elderly Care	NRCan	Urban (Commercial)	roof, asphalt	-79.77646	43.71492
Peel Residential	NRCan	Suburban	grass	-79.76477	43.72273
RH Operations	NRCan	Urban (Municipal)	roof, concrete	-79.40512	43.89737
Rouge	TRCA	Rural	grass	-79.18570	43.80403
Scarborough Residential	NRCan	Suburban	fence, wood	-79.25600	43.70793
Toronto Residential	NRCan	Suburban	grass	-79.45021	43.64464
Downtown/Trinity	EC	Urban (Commercial)	grass	-79.39530	43.66581
Union Station	NRCan	Urban (Industrial)	roof, asphalt	-79.37996	43.64511
United Church	NRCan	Urban (Commercial)	roof, stones, concrete	-79.43285	43.63761
Vaughan Fire 1	NRCan	Urban (Industrial)	roof, gravel	-79.51394	43.79830
Vaughan Fire 2	NRCan	Urban (Industrial)	roof, gravel	-79.54909	43.79336
York University Campus	York U	Urban (Commercial)	grass	-79.50994	43.77529

Appendix II – Land Surface Temperature Maps

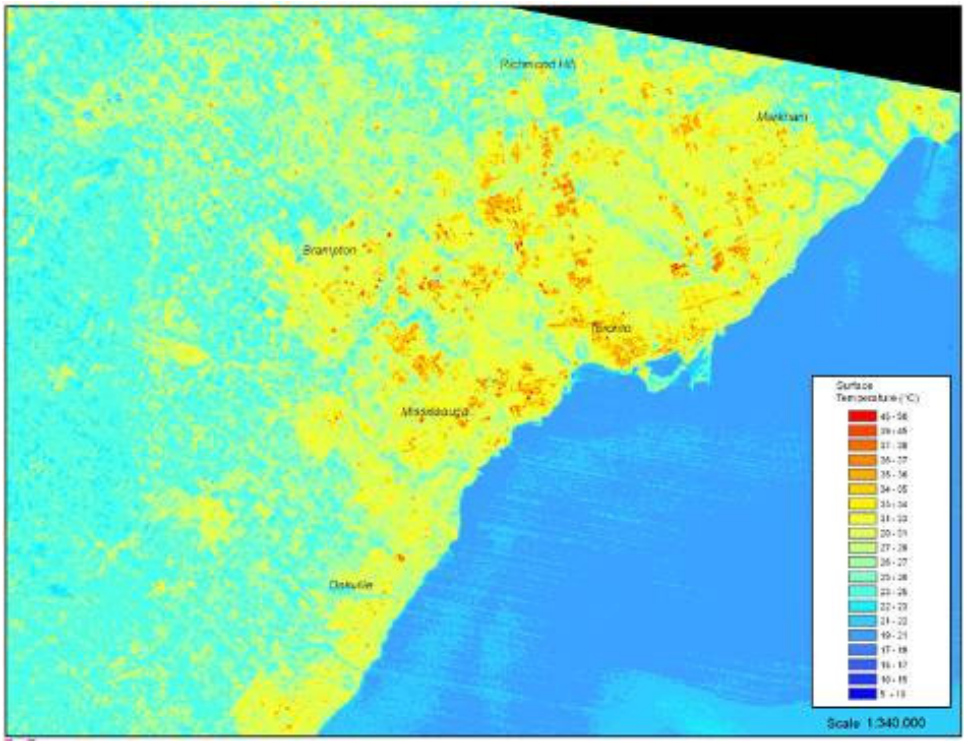

Figure I. Calibrated Land Surface Temperature Map Summer 1990

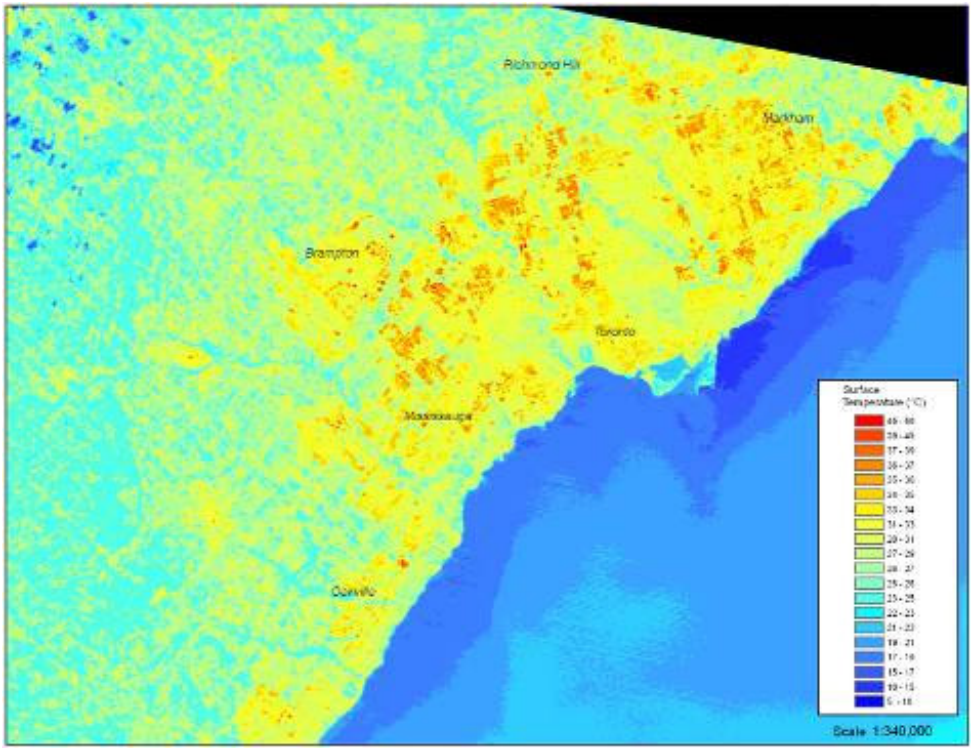

Figure II. Calibrated Land Surface Temperature Map Summer 1994

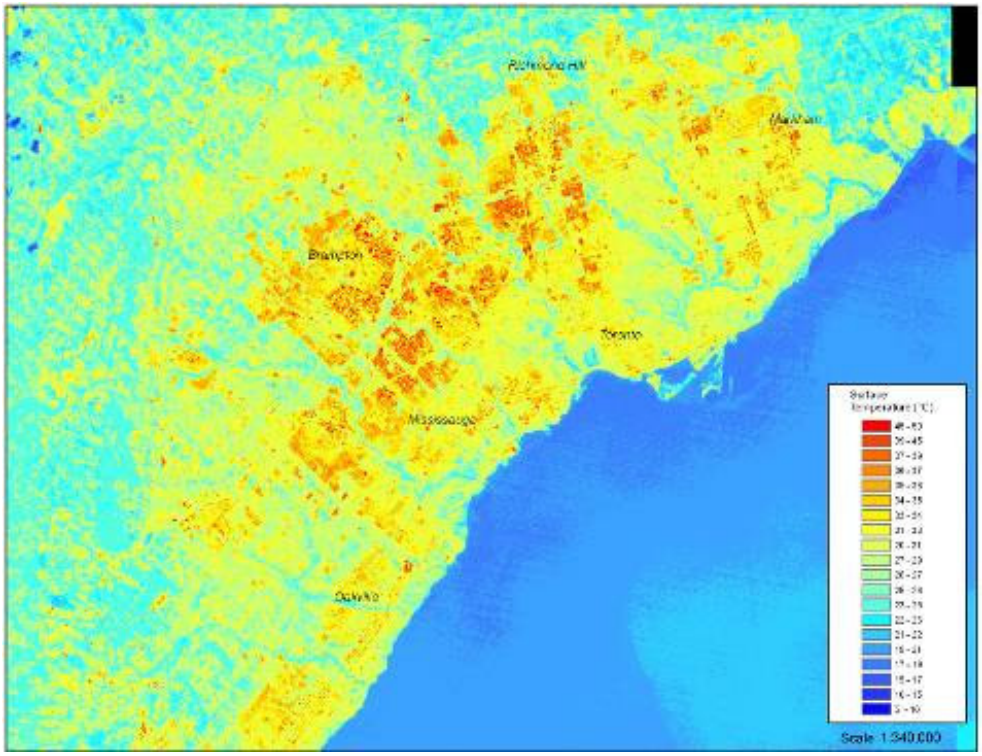

Figure III. Baseline Land Surface Temperature Map Summer 2002

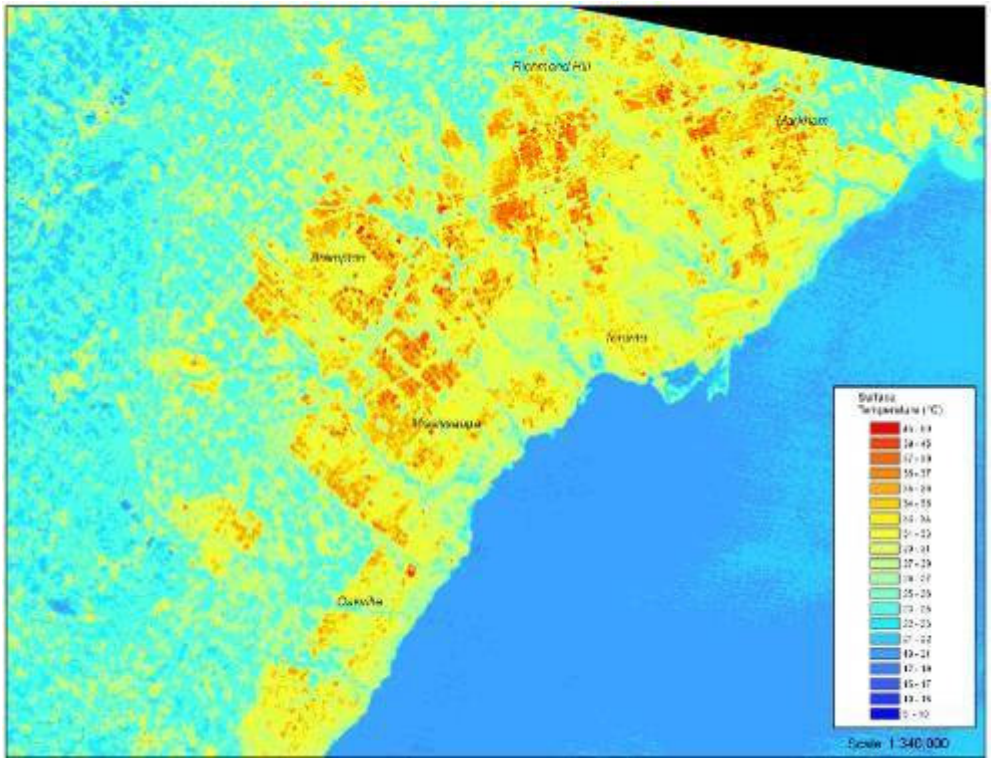

Figure IV. Calibrated Land Surface Temperature Map Summer 2008